



Influence of green solvents on the recovery of cathode active materials from electrode scraps: A comparative study

Mazedur Rahman, Mahmudul Hoq, Hosop Shin*

School of Mechanical Engineering, Purdue University, Indianapolis, IN 46202, USA



ARTICLE INFO

Keywords:

Direct recycling
Lithium-ion batteries
Triethyl phosphate (TEP)
Propylene carbonate (PC)
dihydrolevoglucosanone (Cyrene)

ABSTRACT

Direct recycling of cathode materials from spent Li-ion batteries (LIBs) or electrode scraps necessitates the efficient recovery of active materials from the aluminum foil. The variability in electrode types and recovery processes across previous studies complicates the comparative assessment of the recovery performance of green solvents. In this study, we evaluated the performance of three green solvents—triethyl phosphate (TEP), dihydrolevoglucosanone (Cyrene), and propylene carbonate (PC)—in recovering valuable active materials from industrial-grade cathode scraps. Using ultrasonication, we developed a standardized, energy-efficient recovery process that eliminated the need for conventional stirring and achieved complete cathode delamination from the aluminum foil. Furthermore, we successfully recovered the used green solvents after the process, ensuring their reuse and supporting a circular economy. The recovered materials retained their original morphology, chemical composition, and crystalline structure; however, the presence of surface impurities varied significantly depending on the green solvent used. These impurities had a considerable impact on the electrochemical performance of the recovered materials. TEP and PC yielded high-purity active materials and aluminum foils suitable for reuse or direct recycling, while Cyrene resulted in substantial residues of PVDF/solvent, requiring additional post-processing. Additionally, the recyclability of these green solvents was influenced by their solubility power for PVDF. This study provides valuable insights into the green solvent-based recycling process, laying the groundwork for future sustainable practices in LIB recycling.

1. Introduction

Ongoing environmental and climate concerns have driven a surge in demand for electric vehicles (EVs). As the world moves toward a complete transition to EVs in the transportation sector, Li-ion batteries (LIBs) have become essential components for facilitating this shift. This escalating demand necessitates high-volume production, resulting in a substantial increase in end-of-life (EOL) batteries and electrode scraps. It is estimated that by 2025, approximately 250,000 t of EOL batteries will be retired, prompting the urgent need for environmentally friendly and economically viable recycling and disposal methods [1–5].

Current research efforts have primarily focused on utilizing hydrometallurgical, pyrometallurgical, and direct recycling techniques to retrieve valuable, energy-rich cathode materials from EOL batteries [6–11]. Among these methods, direct recycling has generated significant interest due to its potential to preserve the original structure while replenishing lithium into the damaged crystal structure [12–16]. A critical step in this process involves separating the tightly bonded

cathode materials from the Al foil by breaking the strong bond between the polyvinylidene fluoride (PVDF) binder and the active material or the Al foil. One effective approach is to dissolve or degrade this binder using solvents. While N-methyl-2-pyrrolidone (NMP) and dimethylformamide (DMF) are well-known for their ability to dissolve PVDF, their toxicity and hazardous effects on human health have limited their application in the recycling processes for LIBs.

Recent research efforts have focused on exploring bio-based and environmentally friendly green solvents as alternatives to petroleum-based toxic solvents in LIB recycling processes. Green solvents are typically derived from renewable resources, possess low toxicity, and can reduce the environmental impact of chemical processes. Categories of green solvents include bio-based or biodegradable solvents, ionic liquids (ILs), and deep eutectic solvents (DESs), all of which have been utilized in LIB recycling [17–20]. Bio-based green solvents, such as triethyl phosphate (TEP), Cyrene, γ -valerolactone (GVL), and dimethyl isosorbide (DMI) have demonstrated effectiveness in recovering cathode materials from spent LIBs or electrode scraps [12,13,16,21]. These

* Corresponding author.

E-mail address: shin282@purdue.edu (H. Shin).

solvents displayed excellent PVDF dissolution capabilities at elevated temperatures. Synthetic biodegradable green solvents like propylene carbonate (PC) and ethylene glycol (EG) have also been proposed for cathode recovery processes [14,15]. Furthermore, various IL- and DES-based green solvents (e.g., $[\text{BMIm}][\text{BF}_4]$), $[\text{BMIm}][\text{BF}_6]$, (ChCl:EG), (ChCl:Citric Acid), etc.) have shown great potential for use in cathode recycling due to their unique physicochemical properties, including low vapor pressure, non-flammability, non-toxicity, and biodegradability [22–25]. Notably, DESs have emerged as promising leaching alternatives to inorganic and organic acids for selective metal recovery from spent batteries [19,20]. They have also been used for direct cathode regeneration, allowing for the repair of degraded cathode materials [26].

In previous studies, green solvent-based cathode recovery processes typically involved immersing electrode pieces in a heated solution under continuous mechanical stirring for a prolonged time [12–16,21]. For instance, TEP- and Cyrene-based methods achieved complete cathode delamination at 100 °C after 1 h of stirring, while PC-based methods reached complete delamination at 80 °C in a much shorter time [12–14]. Other green solvents, such as DMI and EG also required high temperatures (> 150 °C) for effective cathode delamination, with the exception of GVL which successfully delaminated spent cathodes at 80 °C using stirring and ultrasonication [15,16,21]. Similarly, ILs and DESs typically demanded higher temperatures (140 °C–150 °C) and exhibited lower delamination efficiency compared to these solvents [22,23,27,28]. ILs and DESs have also been used for the metal recovery of spent cathodes, requiring prolonged high-temperature operation. For instance, DESs such as ChCl:EG and PEG:AA displayed high recovery efficiencies for valuable materials but necessitated extended heating, nearly reaching 200 °C [19,24].

Although previous studies have demonstrated the effectiveness of various green solvents in recovering cathode materials, a systematic comparative assessment of their recovery efficiencies, material characteristics, and electrochemical performance of the recovered cathodes has yet to be conducted. Most prior research has focused on cathode recovery without evaluating the electrochemical performance of the recovered materials. Additionally, the variability of electrode types, processing procedures, and processing parameters across these studies complicates efforts to assess the performance of different green solvents in both recovering cathode materials and preserving the electrochemical properties of those materials. As highlighted in our prior work, cathode recovery efficiency is strongly influenced by the types of electrodes and solvents used [14]. Without employing a consistent process, comparing the effectiveness of different green solvents becomes challenging, hindering progress toward sustainable solvent-based recovery methods.

In this study, we aim to comparatively evaluate the performance of three green solvents (TEP, Cyrene, and PC) in the cathode recovery process by implementing a standardized, ultrasonication-assisted solvent recovery method. By consistently applying this recovery process, we provide a comprehensive understanding of these solvents, which have demonstrated substantial cathode delamination capabilities at specific temperatures [12–14]. Our work seeks not only to identify the most promising solvents but also to assess their impacts on the material characteristics and electrochemical performance of the recovered cathode materials. Ultimately, this study contributes to the development of sustainable recycling practices in the battery industry by offering insights into the optimal utilization of green solvents for cathode recovery.

2. Experimental methods

Materials. A new industrial-grade NMC 532 ($\text{LiNi}_{0.5}\text{Mn}_{0.3}\text{Co}_{0.2}\text{O}_2$, MTI Corporation) was utilized as an electrode scrap in this study. The aerial loading of the electrode was approximately 12.5 mg/cm^2 , with an active material percentage of 94.2 %. TEP (>98 %, Alfa Aesar), Cyrene (>98.5 %, Sigma Aldrich), PC (>99.7 %, anhydrous, Sigma Aldrich), and NMP (>99.5 %, Sigma Aldrich) were used without further

purification for cathode recovery. Pristine NMC 532 powder (MTI Corporation) was also used for comparison.

Cathode Recovery Process. The schematic flowchart of the recovery process is illustrated in Fig. 1, where TEP, Cyrene, and PC were selected as the green solvents for this study. The general characteristics of these solvents are summarized in Table S1.

The industrial-grade electrode sheet was cut into small pieces ($2.54 \times 2.54 \text{ cm}^2$) for the recovery process. A solid/liquid (S/L) ratio of 1:30 (g/ml) was maintained to effectively delaminate the Al foils for the process. First, solvents were heated in a beaker to the desired temperatures: 80 °C for TEP, 90 °C for PC, and 100 °C for Cyrene, which was determined as the optimal temperatures required to delaminate the cathode material within 1 min of follow-up ultrasonication process. After the heating, several electrode pieces were immersed into the heated solvent and left there for 5 min to deactivate the PVDF binder. It should be noted that no mechanical or magnetic stirring was utilized in our experiments. After 5 min, the solution was immediately subjected to short bath-ultrasonication (70 W, <1 min), with each piece being ultrasonicated. During this step, complete cathode delamination occurred, separating the cathode active material, carbon black, and PVDF binder from the Al foil. The resulting black solution was then subjected to centrifugation for 5 min to separate the active material from carbon black and PVDF binder through gravity-based separation. This process allowed the high-density active material to precipitate at the bottom, while the low-density PVDF binder remained dissolved along with the suspended low-density carbon black. After centrifugation, the supernatant consisting of the PVDF and carbon black was filtered, and the sediment (i.e., recovered active material) underwent two additional 5-minute centrifugation cycles using deionized (DI) water. Following this, the recovered active material was initially dried on a hotplate at 100 °C and then further dried overnight in a vacuum oven at 110 °C. After overnight drying, the recovered powder was ground and utilized for materials characterization and electrochemical tests.

Solvent recovery process. After cathode recovery, the resulting, black solution contained a mixture of dissolved PVDF, suspended carbon black, and green solvent. Both PC and Cyrene were recovered using a thermally induced phase separation (TIPS) method. Due to the low solubility power of PVDF in these solvents at room temperature, the phase separation of PVDF occurred as PVDF precipitated upon cooling the solution. After the initial separation step, the remaining mixture was mixed homogeneously on a hotplate at desirable temperatures for 10 min and then immediately centrifuged for 3 cycles until the original color of the solvent became visible. The supernatant was then filtered out, while the PVDF/C black composite precipitated at the bottom (Fig. S1).

For the recovery of TEP, a nonsolvent-induced phase separation (NIPS) was employed using DI water. After adding a few drops of DI water, the black solution was mixed on a hotplate at the desired temperature for 10 min and then subjected to centrifugation. 3 centrifugation cycles of 5 min each were sufficient to recover a mixture of TEP and DI water. This mixture was then processed through a common distillation method to obtain pure TEP.

Materials Characterization. The recovered Al foils and NMC 532 powders were analyzed using various characterization techniques to assess their material characteristics, surface morphology, purity percentage, chemical compositions, and crystal structure. A field emission scanning electron microscopy (FESEM, JEOL JSM-7800F) equipped with energy-dispersive X-ray spectroscopy (EDAX) was used to investigate the surface morphology of the recovered samples. Thermogravimetric Analysis (TGA, SDT-Q600, TA Instruments) was conducted to determine the composition of the recovered powder. The recovered samples were subjected to a heating rate of 5 °C/min in a 50 ml/min argon flow within the temperature range of 25–800 °C to investigate their purity levels. Additionally, inductively coupled plasma mass spectrometry (ICP-MS, PerkinElmer ELAN 6000) analysis was carried out to understand the possibility of transition metals dissolution and lithium leaching during

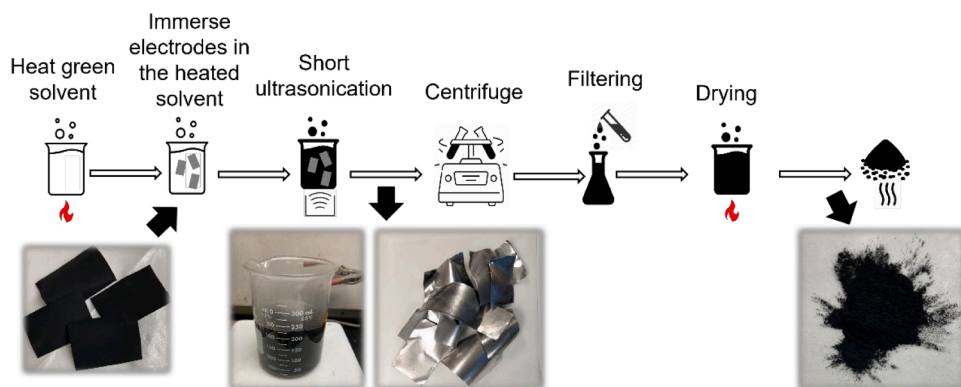


Fig. 1. Schematic flowchart of the green solvent-based cathode recovery process with photo images showing electrode pieces, black solution, recovered Al foils, and recovered active materials.

the recovery process. Powder X-ray diffraction (XRD, Bruker D8 Discover) was employed to examine the crystallinity of the recovered samples, with a scanning rate of $0.5^\circ/\text{min}$ within the 2θ range of $10\text{--}80^\circ$. Fourier-transform infrared spectroscopy (FTIR, PerkinElmer Spectrum 100) was used to analyze the purity of the recovered green solvents.

Electrochemical Measurements. The recovered NMC532 and pristine NMC532 powders were used to make electrodes containing the active material, carbon black (C65, Imerys), and PVDF binder (HSV 900, 8 wt%), in a ratio of 94:3:3 (wt.%). To make the electrode slurry, the powder was hand-grounded with a mortar and pestle and further mixed with carbon black using a planetary centrifugal mixer (Thinky AR-100). Following this, PVDF binder and NMP were added to the mixture for further mixing process. The resulting slurry was coated onto Al foil using a doctor blade. Then, the coated electrode was placed into a vacuum oven for overnight drying at 120°C . The aerial loading was approximately 8 mg/cm^2 .

For electrochemical testing, coin cells were assembled inside an Ar-filled glovebox with oxygen and H_2O levels below 0.1 ppm. These cells were constructed in a half-cell configuration with Li metal as a counter electrode. The electrolyte used in the cells was 1.2 M solution of LiPF_6 in a mixture of ethylene carbonate and ethyl methyl carbonate with a volume ratio of 1:1. After resting the cells for 24 h to ensure proper wetting of the electrolyte with the electrodes, they were subjected to 3 charge/discharge cycles at a C/10 rate using the constant current (CC) charge and discharge protocol. The cells were cycled within a potential range of 3.0–4.3 V (vs. Li/Li^+). Following the formation cycle, electrochemical impedance spectroscopy (EIS) tests were conducted followed by rate tests. The EIS tests were carried out at a fully discharged state

over a frequency range of 500 kHz to 0.1 Hz with a 5 mV amplitude. Long-term cycling performances of all the electrodes were also evaluated after 100 cycles using a C/3 charge and discharge rate.

3. Results and discussion

Ultrasonication-assisted cathode recovery process with green solvents. In our recovery process, cathode delamination from the Al foil occurs via dissolution or degradation of PVDF binder. Our cathode recovery process begins by immersing electrode pieces in heated green solvents. At this stage, solvent molecules penetrate the PVDF structure, causing the polymer chains of PVDF to swell, enhancing the accessibility of reaction pathways for the solvent molecules, and thereby accelerating the disentanglement of the PVDF polymer chains [29]. After the initial interaction between PVDF and the solvent at high temperatures, the pretreated electrode pieces can be rapidly delaminated by a mechanical force such as ultrasonication.

As shown in Fig. 2a, the minimum temperatures necessary for complete cathode delamination revealed that Cyrene required the highest temperature (100°C) among all the green solvents, potentially leading to significant energy consumption during large-scale recovery processes. In contrast, TEP necessitated the lowest temperature (80°C) for complete cathode delamination. In terms of recovery efficiency, PC showed an advantage over other green solvents when the contribution of impurity amount was not considered, achieving approximately 87 % (Fig. 2b). However, the PC-recovered material contained a certain level of impurities (around 0.9 %, Fig. S2), requiring post-processing for impurity removal. Although the impurity level in the PC-recovered

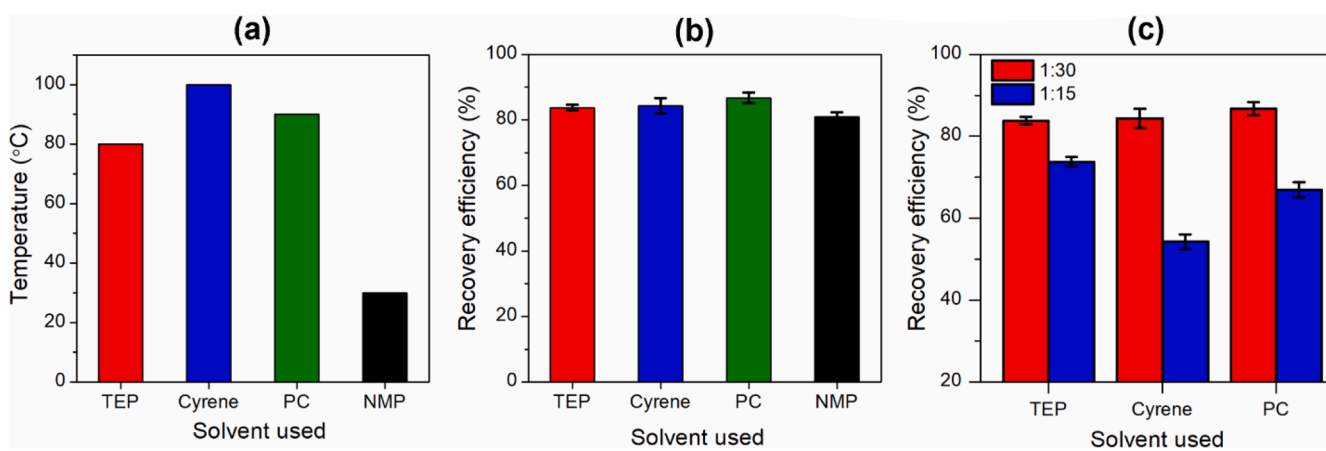


Fig. 2. Comparison of the minimum temperatures required for complete cathode delamination (a), the corresponding cathode recovery efficiencies (b), and the effect of solid-to-liquid ratio (g/ml) on recovery efficiencies (c).

material was lower than that in the Cyrene-recovered material (around 5.5 %, Fig. S2), it was slightly higher compared to TEP and NMP-recovered materials. Even though NMP facilitated cathode material delamination at room temperature, its recovery efficiency was lower compared to green solvents. Overall, TEP demonstrated a high percentage of pure cathode active materials recovered at low temperatures, making it a promising option for direct recycling.

It is important to note that the temperatures employed in our study were significantly lower than those for other green solvents. For example, EG and DMI required temperatures of 160 °C and 150 °C, respectively [15,16], while ILs and DESs generally necessitated temperatures ranging from 120 °C to 190 °C, often accompanied by prolonged heating durations [19,22,23,27,28]. GVL demonstrated effective cathode delamination at 80 °C; the study employed mechanical stirring with spent cathodes, which typically exhibit lower adhesion between the cathode coating and Al foil compared to electrode scraps [21].

Fig. 2c illustrates that the solid-to-liquid (S/L) ratio significantly influenced the recovery efficiency of cathode active materials from electrode scraps. Overall, reducing the solvent amount to a 1:15 S/L ratio decreased the recovery efficiency. Notably, Cyrene exhibited the lowest recovery efficiency at an S/L ratio of 1:15, while TEP maintained good recovery efficiency at the same S/L ratio. This indicates that the TEP-based recovery is less sensitive to solvent volume compared to PC and Cyrene. Consequently, this suggests that the TEP-based recovery could reduce solvent consumption, thereby lowering the overall cost of the process.

In our experiments, an S/L ratio of 1:30 was optimized to ensure high cathode recovery efficiency for all the green solvents studied. This ratio falls within the range used in previous studies, which typically reported S/L ratios from 1:10 to 1:40 [15,16,21]. However, it is important to note that the optimal S/L ratio is strongly influenced by the specifics of the recovery processes and various parameters such as heating temperature and duration.

Materials characterization of recovered Al foils, cathode active materials, and green solvents. Fig. 3 displays SEM images and associated EDAX spectra of the Al foils obtained from the recovery process using different solvents. SEM/EDAX analysis revealed that the purity levels of the Al foils recovered by TEP and PC were higher compared to the NMP-recovered Al foil, achieving approximately 94 % and 88 %, respectively. In contrast, the Cyrene-recovered Al foil exhibited the lowest purity level, approximately 76 %. The TEP-recovered Al foil showed the lowest amount of transition metals (TMs), while the Cyrene-recovered Al foil showed the highest. The weight ratio of TMs represents the presence of active cathode materials (i.e., NMC particles) on the Al foils. Among all the green solvents, TEP demonstrated its excellence in effectively delaminating the cathode active material.

Notably, the Al foil recovered by Cyrene showed the highest amount of C and O compared to any other solvents. The percentages of C and O on the Al surface can be attributed to the presence of residual organic solvent molecules, formed by the cross-linking of the hydrogen bonds during the recovery process, as well as reprecipitated PVDF/Cyrene residues [16,30]. As previously reported, PVDF dissolution in Cyrene is temperature-sensitive, requiring a constant high temperature throughout the entire recovery process [13,31]. Otherwise, dissolved PVDF can be reprecipitated on the cathode material and Al surfaces. Our results reaffirm that using Cyrene necessitates continuous heating throughout the entire cathode recovery process, potentially leading to higher energy consumption than other green solvents.

As shown in SEM images, damaged spots or pits in the Al foil were visible in all the Al foil samples. Further analysis revealed them to be a product of Al and O, indicating oxidation of the Al foil after the delamination process. The pits could also be caused by the calendaring process during manufacturing, which compresses the electrode for better adhesion and higher loading [32].

Fig. 4 exhibits the SEM images of the cathode active materials delaminated from the Al foils using different solvents. We compared the

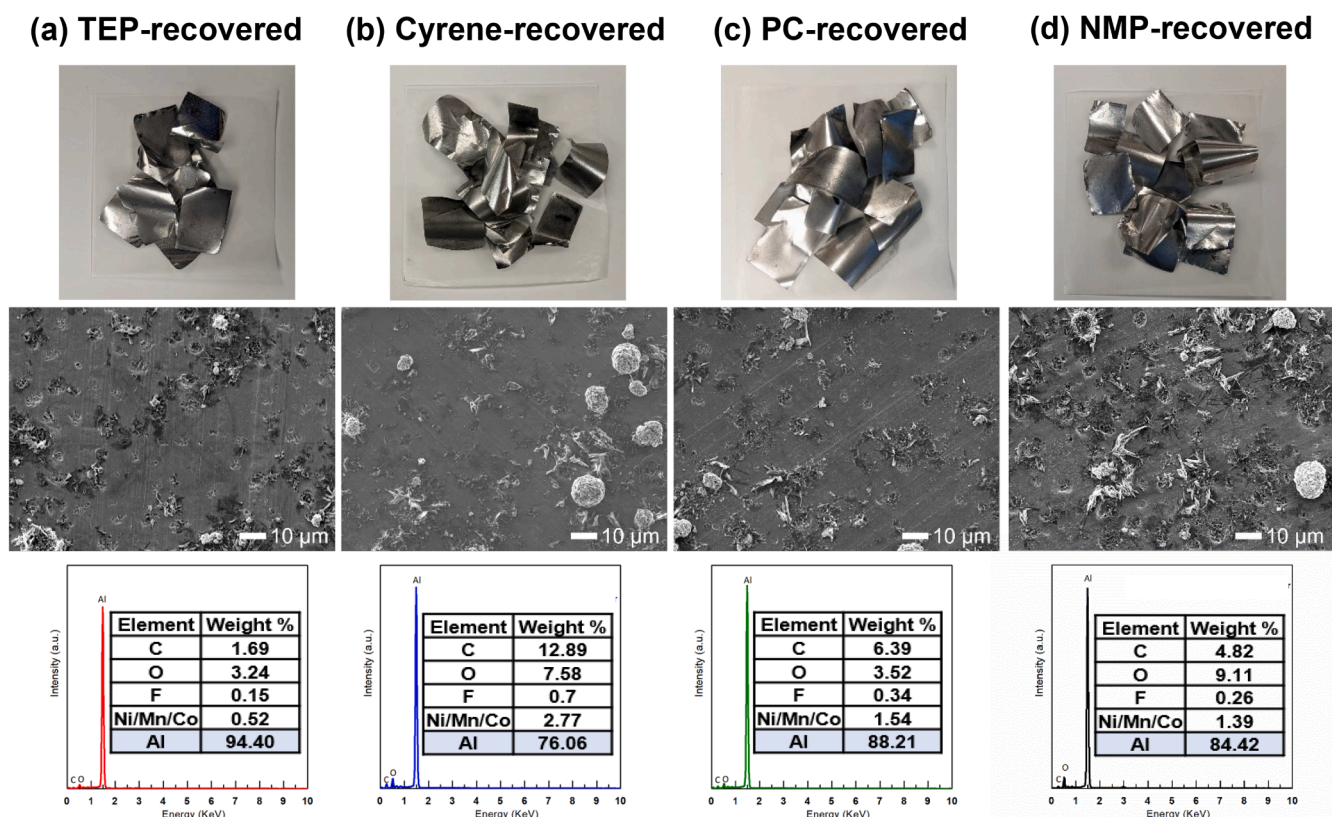


Fig. 3. Comparison of the Al foils recovered by TEP (a), Cyrene (b), PC (c), and NMP (d) solvents using photos and SEM/EDAX analyses.

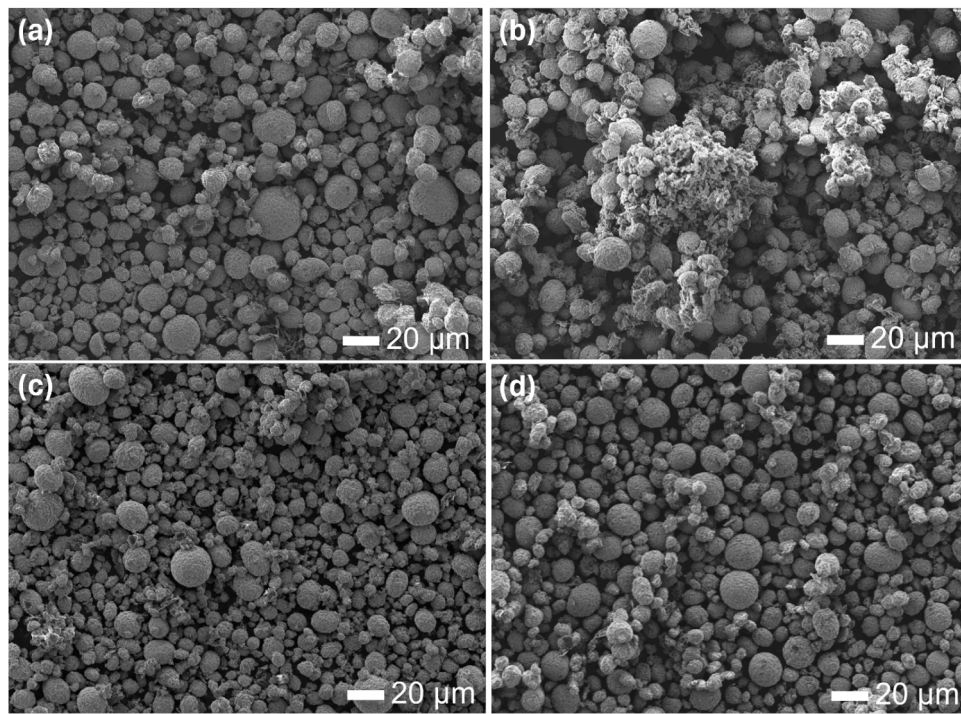


Fig. 4. SEM images of cathode materials recovered by, NMP (a), Cyrene (b), TEP (c), and PC (d) solvents.

particle morphology of the recovered cathode powders with each other and with manually scraped-off cathode powder. Figure S3 shows that the scraped-off cathode powder failed to maintain its original particle morphology. Most secondary NMC particles were not visible in the sample because they were still strongly bonded with carbon black and PVDF binder. This highlights the challenge of obtaining pure cathode active materials through mechanical delamination.

In contrast, the solvent-based process recovered cathode powders with well-defined secondary NMC particles, displaying higher TM ratios compared to the manually scraped-off cathode powder, except for the Cyrene-recovered sample, as depicted in Figs. 4 and S4. The higher TM ratios demonstrated that TEP and PC-recovered samples had fewer impurities, such as carbon black and PVDF binder, than the scrape-off sample.

Our process, which included a simple heating step followed by short-duration ultrasonication, ensured the preservation of the original particle morphology while significantly reducing the presence of carbon black and PVDF binder. It is worth noting that prolonged mechanical or magnetic stirring with extended ultrasonication can lead to decreased delamination efficiency, particle morphology damage, and the introduction of Al debris into the recovered active materials [33,34]. However, the active materials recovered using all the green solvents showed no Al peaks in the EDAX element mapping, indicating the absence of Al impurities (Fig. S4). This absence is primarily attributed to the short heating and ultrasonication. The lack of Al impurities was further confirmed by the ICP-MS data (Fig. S7).

TEP and PC-recovered samples maintained their original particle morphology, exhibiting particle sizes and distributions similar to those of the NMP-recovered sample. However, unlike the others, the Cyrene-recovered sample displayed numerous particle agglomerations with charged-up effects (bright regions in Fig. S4) across its surface (Figs. 4 and S4). Substances composed of C and O were widely found in the recovered sample and adhered to particle surfaces, causing severe agglomeration and changes in surface properties (Figs. S4 and S5). The formation of this substance is most likely caused by both thermal-induced and nonsolvent-induced phase separation mechanisms.

It is worth noting that our separation process involved one centrifuge

cycle with green solvents followed by two cycles with DI water. Although the supernatant containing the majority of PVDF and carbon black was expected to be removed after the first centrifuge cycle, the sediment can retain PVDF/Cyrene residues on the active material surface. When the sediment was in contact with DI water at room temperature during subsequent centrifuge cycles, the PVDF/Cyrene residue solution separated into two distinct phases: a PVDF-rich phase and a Cyrene-rich phase, which can be the origin of the impurity substance observed in the Cyrene-recovered sample. The absence of F in the EDAX mapping of the impurity substance suggests that its characteristics differed from the original PVDF binder.

Interestingly, this type of substance was not much observed in TEP and PC-recovered samples, despite the identical process applied to all samples. This implies that the reduction in solvent-polymer affinity induced by water, triggering phase separation, is more pronounced for Cyrene compared to other green solvents. Further post-treatment steps may be pivotal for advancing Cyrene-based direct cathode recovery processes.

The EDAX analysis (Fig. S4) further revealed that the initial 5:3:2 ratio of Ni, Mn, and Co was preserved in all recovered active materials, suggesting that no leaching of transition metals occurred. This finding aligns with our ICP-MS data (Fig. S7). Moreover, the presence of C in the recovered samples can be attributed not only to residual carbon black but also PVDF/solvent residues.

To quantify and compare impurities in the recovered samples, TGA was conducted on all samples, including pristine NMC 532 powder and scraped NMC 532 powder, as depicted in Fig. 5a. Except for Cyrene, both TEP and PC-recovered powders exhibited overall less weight loss (0.61 % and 1.25 %, respectively) than the scraped-off powder (5.72 %), demonstrating the effectiveness of our recovery process using these green solvents. Pristine NMC powder showed no visible weight loss in the temperature range, indicating the perfect purity of pristine NMC powder. In contrast, the scraped powder displayed three distinct stages of weight loss: the first around 280–500 °C, followed by a second at 500–630 °C, and a third after 630 °C. The first weight loss stemmed from PVDF binder decomposition [35–37]. The subsequent stages originated from carbon black and active material decomposition, respectively

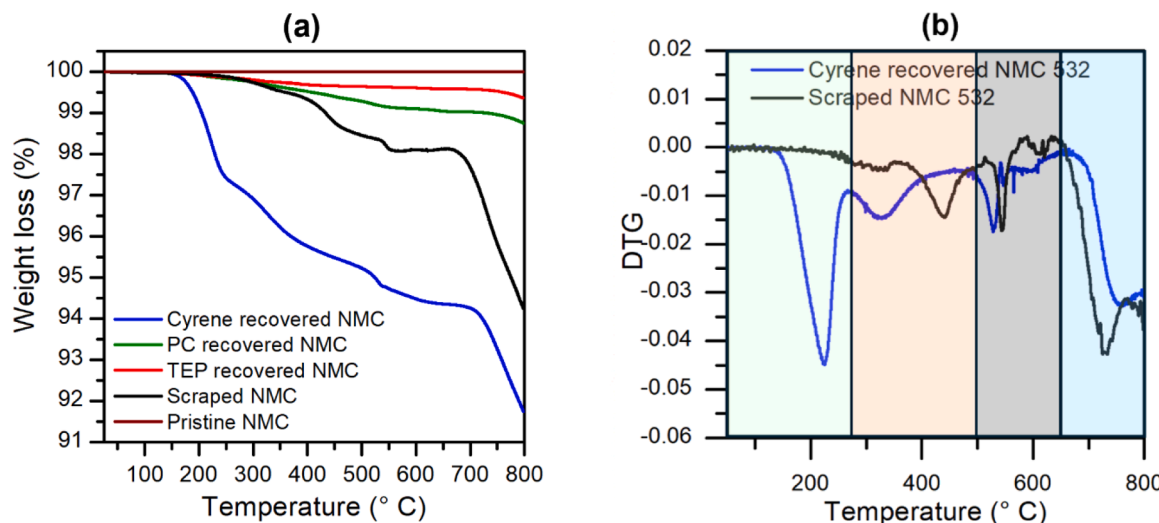


Fig. 5. Comparison of TGA of the cathode materials recovered by using green solvents and pristine NMC (a); DTG comparison between Cyrene recovered and manually scraped cathode powders (b).

[38–40]. Both TEP and PC showed significantly fewer weight losses, indicating effective removal of PVDF binder and carbon black using these solvents, consistent with the SEM/EDAX analysis discussed before. Among all the green solvents, TEP performed the best, recovering high-purity active materials.

In contrast, the Cyrene-recovered powder exhibited a higher percentage of weight loss (8.23 %) compared to all other samples, with an additional stage of weight loss between 120 and 280 °C, where a significant weight loss occurred (2.85 %) (Fig. 5a and Table S2). To investigate the origin of this loss, a separate TGA test was performed on Cyrene solvent. As shown in Figure S6, the Cyrene solvent completely evaporated even before 200 °C, suggesting that the weight loss was not due to any Cyrene residues on the sample surface. Further analysis of the Cyrene-recovered sample using derivative thermogravimetric analysis (DTG) revealed two distinct peaks under 500 °C: one around 220 °C, absent in the scraped sample, and the other around 330 °C, lower than the PVDF decomposition temperature (400–510 °C) observed for the scraped sample (Fig. 5b). These peaks likely correspond to a Cyrene-rich phase and a PVDF-rich phase of the PVDF/Cyrene residue remaining on the active material surface, respectively, considering PVDF's melting point (177 °C) and the phase separation mechanism of the PVDF/Cyrene solution mixture.

It should be noted that the decomposition of the active material occurred at earlier temperatures for both the scraped and Cyrene-recovered samples compared to both TEP and PC-recovered samples. This suggests a higher proportion of carbon black in the Cyrene-recovered sample than in TEP and PC-recovered samples, accelerating NMC decomposition at lower temperatures. Previous reports have noted that the presence of carbon black accelerates NMC decomposition, contributing to the thermal instability of NMC [14].

Fig. 6 shows the XRD patterns of the scraped powder and the solvent-recovered powders. All samples exhibited similar diffraction peaks to the scraped NMC 532 powder, indexed to a R3m space group with an α -NaFeO₂ layered rhombohedral structure. No significant peak shifting or broadening was observed, confirming the preservation of the crystalline structure and the absence of defects in the recovered cathode powders. The intensity ratio of the (003)/(104) peaks and a low value of $R = (I_{012} + I_{006}) / I_{101}$ (Table 1) indicates negligible Ni-Li cation mixing and good separation between Li and TM ions, ensuring the stability of the crystal structures [41,42].

A previous report suggested the possibility of Cyrene-induced Li⁺leaching from cathode materials [13]. Similarly, the EG-based recovery process also exhibited some Li leaching after recovery, possibly

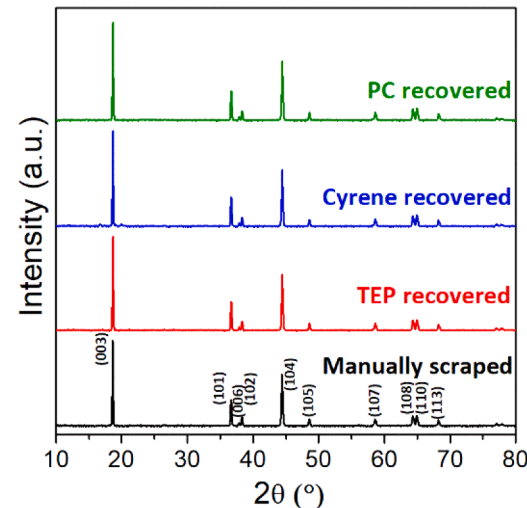


Fig. 6. XRD patterns of the recovered cathode powders.

Table 1
XRD peak analysis of manually scraped and green solvent-recovered samples.

	Manually scraped NMC 532	TEP-recovered NMC 532	Cyrene-recovered NMC 532	PC-recovered NMC 532
I_{003}/I_{104}	1.65	1.64	1.69	1.63
Distance	0.61	0.63	0.61	0.63
108/110				
$R = (I_{012} + I_{006}) / I_{101}$	0.44	0.43	0.41	0.43

occurring during the separation or washing of the cathode active materials [15]. However, our ICP-MS analysis demonstrated that all samples maintained a consistent molar ratio of Li, Ni, Mn, and Co (Fig. S7), similar to that of the NMP-recovered sample. This indicates that our rapid recovery process effectively prevented Li or TM leaching during the process, thereby preserving the original chemical composition of the active materials. Alternatively, the discrepancy between our results and the previous report may stem from the difference in the active material used for the solvent-based recovery process. Ni-rich NMCs are known to

be sensitive to moisture and air, which may require a more delicate process to avoid any Li leaching during the recovery process.

To promote a circular economy and minimize the waste and environmental impact of the green solvent-based cathode recovery process, it is also critical to evaluate the recyclability of green solvents used in the process. As outlined in the method section, the solvent recycling method was strongly affected by the characteristics of green solvents. Both PC and Cyrene solvents were recovered by a similar TIPS-based process, while TEP required a distinct NIPS-based approach for solvent recovery. Our FTIR analysis revealed that all the recovered solvents maintained their original chemical structures. Figure S8 demonstrates that the FTIR band positions of the recovered TEP, Cyrene, and PC closely matched those of the corresponding pure solvents. The relative positions of the key characteristic peaks remained stable, with no significant shifts or broadening observed. This confirms that the solvents recovered retained the same level of purity as the pristine solvents and can be reused for future recovery of cathode active materials or other applications.

Electrochemical performance of recovered cathode active materials. We conducted various electrochemical tests to evaluate the impact of different green solvents on the electrochemical performance of the recovered cathodes. As highlighted in the introduction, while previous studies have explored various aspects of cathode recovery, the electrochemical performance of recovered materials has been largely overlooked, with only a few studies addressing it. It is important to note that the primary objective of direct cathode recovery from electrode scars is to recycle or directly reuse the recovered cathode in new electrode manufacturing. Therefore, assessing the electrochemical properties of the recovered materials is essential.

In our study, the NMP-recovered cathode served as the baseline for comparison. We also compared the electrochemical properties of the

recovered samples with pristine NMC samples for reference. (Fig. S9). Fig. 7a illustrates that cathodes recovered with TEP and PC displayed discharge capacities similar to that of the NMP-recovered cathode, with charge-discharge curves comparable to the baseline. However, the Cyrene-recovered cathode showed a lower discharge capacity, approximately 25 % less than those of TEP and PC-recovered cathodes. Consistent with a previous study, the decrease in discharge capacity can be attributed to the presence of PVDF/Cyrene residue impurity in the Cyrene-recovered powder, as evidenced by TGA [13]. This impurity resulted in a smaller amount of active material in the recovered cathode, thus reducing the discharge capacity. Furthermore, excessive impurities can have a negative impact on active material utilization by altering the porosity, tortuosity, and wetting properties of the desired electrode microstructure [43–45].

As expected, the first cycle Coulombic efficiency of the Cyrene-recovered cathode was the lowest (Fig. 7b), potentially due to increased side reactions, interfacial resistance, and altered electrode properties induced by the reprecipitated PVDF/Cyrene residue [46]. PC and NMP-recovered cathodes showed the first cycle Coulombic efficiency similar to the original cathode, showcasing their advantages over other green solvents.

EIS tests revealed that PC-recovered cathodes exhibited the lowest impedance, while Cyrene-recovered cathodes had the highest (Fig. 7c). As reported in previous studies, the plasticizer effect of PC with PVDF could contribute to reducing the overall impedance of the electrode by enhancing Li-ion transport at the cathode/electrolyte interface [47–50]. This observation may also explain why PC-recovered cathodes displayed better rate capability compared to those recovered with other green solvents (Fig. 7d). The high impedance of Cyrene-recovered cathodes was possibly due to the PVDF/Cyrene residue, which could lead to poor

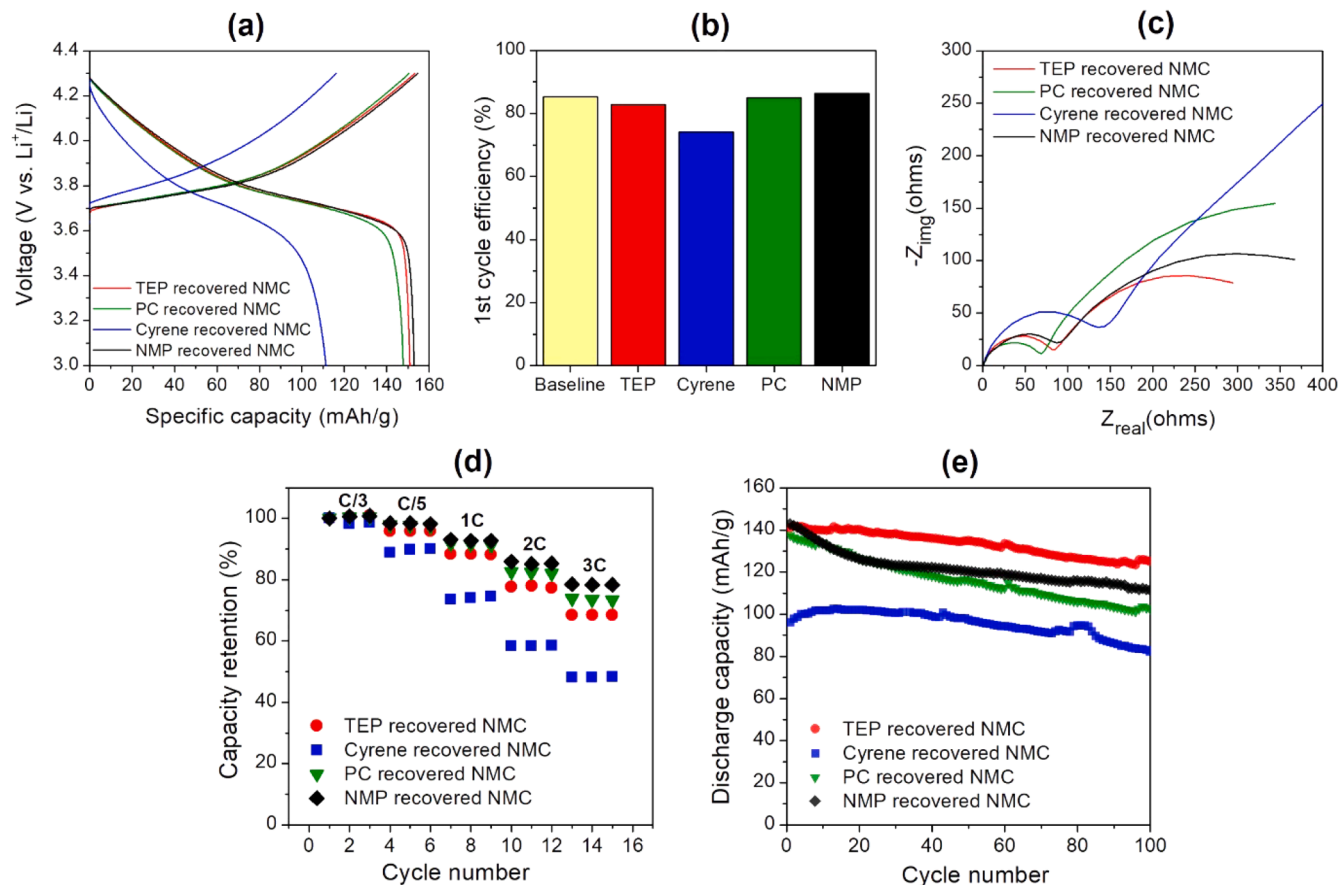


Fig. 7. Comparison of (a) charge-discharge curves at the end of the formation cycle (C/10 rate), (b) first cycle Coulombic efficiencies, (c) Nyquist plots after the formation cycle, (d) rate capabilities, and (e) cycle performances (C/3 rate) of the recovered cathodes.

wettability and Li-ion transport at the cathode/electrolyte interface. This hypothesis finds further support in the higher voltage spike and overpotential observed during the first charge cycle compared to other recovered cathodes (Fig. S10). When cathode materials exhibit poor wettability, electrolyte penetration into the electrode pores can be limited. As a result, the effective electrochemical surface area may be reduced, resulting in increased resistance and overpotential. Additionally, the presence of PVDF/Cyrene residue may impede the initial Li-ion deintercalation process at the cathode/electrolyte interface.

All green solvent-recovered cathodes exhibited stable cycle performance similar to the baseline NMC-recovered cathode (Fig. 7e). Interestingly, TEP-recovered cathodes showed better capacity retention than the NMC-recovered cathode, maintaining 88 % of the initial capacity after 100 cycles. PC-recovered cathodes displayed capacity retention of 75 %, comparable to NMP-recovered cathodes (77 %). Cyrene-recovered cathodes also demonstrated stable cycle performance with an initial increase in capacity at the beginning of cycles. This initial increase in discharge capacity may be attributed to the improved wettability of the recovered cathode upon cycling. However, the reversible capacity of Cyrene-recovered cathodes was significantly lower than that of other recovered cathodes, possibly due to the presence of PVDF/Cyrene residue in Cyrene-recovered cathodes.

In summary, the electrochemical properties of the recovered cathode materials were strongly correlated with the quantity and characteristics of the impurities present. Consistent with findings from previous studies on solvent-based recovered materials, the reversible capacity of the recovered cathode materials was influenced by the amount of impurities as their weight contributed to the weight of the active materials [12–15]. Other electrochemical properties, including the first cycle efficiency, interfacial impedance, and rate capability were affected not only by the quantity of impurities but also by their characteristics, which were determined by the green solvent used.

4. Conclusions

This study demonstrates the effectiveness of green solvents—TEP, PC, and Cyrene—for the efficient recovery of cathode active materials from electrode scraps. Using an ultrasonication-assisted recovery process, we achieved complete cathode delamination from Al foil at low temperatures and within a short timeframe, eliminating the need for mechanical stirring and enhancing energy efficiency.

Our findings reveal a strong correlation between the purity and electrochemical performance of the recovered cathode materials and the choice of green solvent. TEP and PC yielded high-purity active materials suitable for reuse or direct recycling, while Cyrene resulted in significant residues of PVDF/Cyrene that required additional post-processing. Furthermore, the presence and characteristics of impurities varied depending on the solvent used, substantially affecting key electrochemical properties such as reversible capacity, first cycle efficiency, interfacial impedance, cycle performance, and rate capability.

The study also highlights that the solvent recovery methods are influenced by the characteristics of the green solvents: both PC and Cyrene were recovered using a TIP-based process, while TEP required a distinct NIPS-based approach. The recovered solvents maintained the same level of purity as the pristine solvent, confirming their recyclability for future cathode recovery or other applications.

Overall, our research provides valuable insights into the green solvent-based recycling process, laying the groundwork for future sustainable practices in LIB recycling. Further investigations should focus on developing purification processes to remove residual impurities from the recovered materials and implementing the green solvent recovery process into direct cathode regeneration.

CRediT authorship contribution statement

Mazedur Rahman: Writing – original draft, Methodology,

Investigation, Formal analysis. **Mahmudul Hoq:** Writing – review & editing, Methodology, Investigation, Formal analysis. **Hosop Shin:** Writing – review & editing, Supervision, Resources, Project administration, Methodology, Investigation, Funding acquisition, Formal analysis, Conceptualization.

Declaration of competing interest

The authors declare that they have no known competing financial interests or personal relationships that could have appeared to influence the work reported in this paper.

Acknowledgments

The authors acknowledge the financial support provided by the National Science Foundation under Grant No. 2138553. This work is also partially supported by the Samsung Advanced Institute of Technology through the Samsung Global Research Outreach (GRO) program. The authors extend our sincere thanks to Dr. Dawoon Jang and Dr. Jung-Hyun Kim at The Ohio State University for their generous assistance with the ICP-MS analysis.

Supplementary materials

Supplementary material associated with this article can be found, in the online version, at [doi:10.1016/j.electacta.2024.145225](https://doi.org/10.1016/j.electacta.2024.145225).

Data availability

Data will be made available on request.

References

- [1] K.M. Winslow, S.J. Laux, T.G. Townsend, A review on the growing concern and potential management strategies of waste lithium-ion batteries, *Resour. Conserv. Recycl.* 129 (2018) 263–277, <https://doi.org/10.1016/j.resconrec.2017.11.001>.
- [2] Y. Bai, N. Muralidharan, Y.K. Sun, S. Passerini, M. Stanley Whittingham, I. Belharouak, Energy and environmental aspects in recycling lithium-ion batteries: concept of Battery identity global passport, *Mater. Today* 41 (2020) 304–315, <https://doi.org/10.1016/j.mattod.2020.09.001>.
- [3] L. Gaines, K. Richa, J. Spangenberger, Key issues for Li-ion battery recycling, *MRS Energy Sustain* 5 (2018) 12, <https://doi.org/10.1557/mre.2018.13>.
- [4] G. Harper, R. Sommerville, E. Kendrick, L. Driscoll, P. Slater, R. Stolkin, A. Walton, P. Christensen, O. Heidrich, S. Lambert, A. Abbott, K. Ryder, L. Gaines, P. Anderson, Recycling lithium-ion batteries from electric vehicles, *Nature* 575 (2019) 75–86, <https://doi.org/10.1038/s41586-019-1682-5>.
- [5] M. Chen, X. Ma, B. Chen, R. Arsenault, P. Karlson, N. Simon, Y. Wang, Recycling end-of-life electric vehicle lithium-ion batteries, *Joule* 3 (2019) 2622–2646, <https://doi.org/10.1016/j.joule.2019.09.014>.
- [6] N. Vieceli, C.A. Nogueira, C. Guimaraes, M.F.C. Pereira, F.O. Durão, F. Margarido, Hydrometallurgical recycling of lithium-ion batteries by reductive leaching with sodium metabisulphite, *Waste Manag* 71 (2018) 350–361, <https://doi.org/10.1016/j.wasman.2017.09.032>.
- [7] Y. Yao, M. Zhu, Z. Zhao, B. Tong, Y. Fan, Z. Hua, Hydrometallurgical processes for recycling spent lithium-ion batteries: a critical review, *ACS Sustain. Chem. Eng.* 6 (2018) 13611–13627, <https://doi.org/10.1021/acssuschemeng.8b03545>.
- [8] S. Windisch-Kern, A. Holzer, C. Ponak, H. Raupenstrauch, Pyrometallurgical lithium-ion-battery recycling: approach to limiting lithium slagging with the induced reactor concept, *Processes* 9 (2021) 84, <https://doi.org/10.3390/pr9010084>.
- [9] M. Zhou, B. Li, J. Li, Z. Xu, Pyrometallurgical Technology in the Recycling of a Spent Lithium Ion Battery: evolution and the Challenge, *ACS EST Eng* 1 (2021) 1369–1382, <https://doi.org/10.1021/acsestengg.1c00067>.
- [10] T.O. Folayan, A.L. Lipson, J.L. Durham, H. Pinegar, D. Liu, L. Pan, Direct recycling of blended cathode materials by froth flotation, *Energy Technol* 9 (2021) 2100468, <https://doi.org/10.1002/ente.202100468>.
- [11] H. Shin, R. Zhan, K.S. Dhindsa, L. Pan, T. Han, Electrochemical performance of recycled cathode active materials using froth flotation-based separation process, *J. Electrochem. Soc.* 167 (2020) 020504, <https://doi.org/10.1149/1945-7111/ab6280>.
- [12] Y. Bai, R. Essehl, C.J. Jafta, K.M. Livingston, I. Belharouak, Recovery of cathode materials and aluminum foil using a green solvent, *ACS Sustain. Chem. Eng.* 9 (2021) 6048–6055, <https://doi.org/10.1021/acssuschemeng.1c01293>.
- [13] Y. Bai, W.B. Hawley, C.J. Jafta, N. Muralidharan, B.J. Polzin, I. Belharouak, Sustainable recycling of cathode scraps via Cyrene-based separation, *Sustain.*

Mater. Technol. 25 (2020) e00202, <https://doi.org/10.1016/j.susmat.2020.e00202>.

[14] Md.S.A. Bhuyan, H. Shin, Green recovery of cathode active materials from li-ion battery electrode scraps using propylene carbonate: a novel approach for direct recycling, ACS Sustain. Chem. Eng. 11 (2023) 10677–10687, <https://doi.org/10.1021/acssuschemeng.3c01278>.

[15] Y. Bai, N. Muralidharan, J. Li, R. Essehli, I. Belharouak, Sustainable direct recycling of lithium-ion batteries via solvent recovery of electrode materials, ChemSusChem 13 (2020) 5664–5670, <https://doi.org/10.1002/cssc.202001479>.

[16] O. Buken, K. Mancini, A. Sarkar, A sustainable approach to cathode delamination using a green solvent, RSC Adv 11 (2021) 27356–27368, <https://doi.org/10.1039/DRA04922D>.

[17] E.A. Othman, A.G.J. Van Der Ham, H. Miedema, S.R.A. Kersten, Recovery of metals from spent lithium-ion batteries using ionic liquid [P8888][Oleate], Sep. Purif. Technol. 252 (2020) 117435, <https://doi.org/10.1016/j.seppur.2020.117435>.

[18] G. Zante, A. Masmoudi, R. Barillon, D. Trébouet, M. Boltoeva, Separation of lithium, cobalt and nickel from spent lithium-ion batteries using TBP and imidazolium-based ionic liquids, J. Ind. Eng. Chem. 82 (2020) 269–277, <https://doi.org/10.1016/j.jiec.2019.10.023>.

[19] Y. Chen, Y. Wang, Y. Bai, M. Feng, F. Zhou, Y. Lu, Y. Guo, Y. Zhang, T. Mu, Mild and efficient recovery of lithium-ion battery cathode material by deep eutectic solvents with natural and cheap components, Green Chem. Eng. 4 (2023) 303–311, <https://doi.org/10.1016/j.gce.2022.06.005>.

[20] C. Ma, M. Svärd, K. Forsberg, Recycling cathode material LiCo_{1/3}Ni_{1/3}Mn_{1/3}O₂ by leaching with a deep eutectic solvent and metal recovery with antisolvent crystallization, Resour. Conserv. Recycl. 186 (2022) 106579, <https://doi.org/10.1016/j.resconrec.2022.106579>.

[21] Z. Fang, Q. Duan, Q. Peng, Z. Wei, L. Jiang, J. Sun, Q. Wang, A sustainable delamination method to completely separate spent cathode foils via biomass-derived γ -valerolactone, Green Chem. 25 (2023) 1546–1558, <https://doi.org/10.1039/D2GC04436F>.

[22] X. Zeng, J. Li, Innovative application of ionic liquid to separate Al and cathode materials from spent high-power lithium-ion batteries, J. Hazard. Mater. 271 (2014) 50–56, <https://doi.org/10.1016/j.jhazmat.2014.02.001>.

[23] Y. Zhao, Q. Su, W. Zhang, W. Zhang, Y. Bao, M. Guan, Y. Zhuang, Research on the separation process of positive electrode active material and aluminum foil, J. Ind. Eng. Chem. 134 (2024) 281–288, <https://doi.org/10.1016/j.jiec.2023.12.058>.

[24] M.K. Tran, M.T.F. Rodrigues, K. Kato, G. Babu, P.M. Ajayan, Deep eutectic solvents for cathode recycling of Li-ion batteries, Nat. Energy 4 (2019) 339–345, <https://doi.org/10.1038/s41560-019-0368-4>.

[25] N. Peeters, K. Binnemans, S. Riaño, Solvometallurgical recovery of cobalt from lithium-ion battery cathode materials using deep-eutectic solvents, Green Chem. 22 (2020) 4210–4221, <https://doi.org/10.1039/D0GC00940G>.

[26] J. Wang, Q. Zhang, J. Sheng, Z. Liang, J. Ma, Y. Chen, G. Zhou, H.M. Cheng, Direct and green repairing of degraded LiCoO₂ for reuse in lithium-ion batteries, Natl. Sci. Rev. 9 (2022) nwac097, <https://doi.org/10.1093/nsr/nwac097>.

[27] M. Wang, Q. Tan, L. Liu, J. Li, Efficient separation of aluminum foil and cathode materials from spent lithium-ion batteries using a low-temperature molten salt, ACS Sustain. Chem. Eng. 7 (2019) 8287–8294, <https://doi.org/10.1021/acssuschemeng.8b06694>.

[28] M. Wang, Q. Tan, L. Liu, J. Li, A low-toxicity and high-efficiency deep eutectic solvent for the separation of aluminum foil and cathode materials from spent lithium-ion batteries, J. Hazard. Mater. 380 (2019) 120846, <https://doi.org/10.1016/j.jhazmat.2019.120846>.

[29] J.E. Marshall, A. Zhenova, S. Roberts, T. Petchey, P. Zhu, C.E.J. Dancer, C. R. McElroy, E. Kendrick, V. Goodship, On the Solubility and Stability of Polyvinylidene Fluoride, Polymers 13 (2021) 1354, <https://doi.org/10.3390/polym13091354>.

[30] T. Marino, F. Russo, A. Figoli, The formation of polyvinylidene fluoride membranes with tailored properties via vapour/non-solvent induced phase separation, Membranes 8 (2018) 71, <https://doi.org/10.3390/membranes8030071>.

[31] H. Zhou, B. Pei, Q. Fan, F. Xin, M.S. Whittingham, Can greener cyrene replace NMP for electrode preparation of NMC 811 cathodes? J. Electrochem. Soc. 168 (2021) 040536 <https://doi.org/10.1149/1945-7111/abf87d>.

[32] A.C. Ngandjou, T. Lombardo, E.N. Primo, M. Chouchane, A. Shodiev, O. Arcelus, A.A. Franco, Investigating electrode calendering and its impact on electrochemical performance by means of a new discrete element method model: towards a digital twin of Li-Ion battery manufacturing, J. Power Sources 485 (2021) 229320, <https://doi.org/10.1016/j.jpowsour.2020.229320>.

[33] M. Jafari, M.M. Torabian, A. Bazargan, A facile chemical-free cathode powder separation method for lithium ion battery resource recovery, J. Energy Storage 31 (2020) 101564, <https://doi.org/10.1016/j.est.2020.101564>.

[34] M. Zhou, K. Liu, M. Wei, J. Zhang, S. Chen, W. Cheng, Recovery of lithium iron phosphate by specific ultrasonic cavitation parameters, Sustainability 14 (2022) 3390, <https://doi.org/10.3390/su14063390>.

[35] J. Mao, J. Li, Z. Xu, Coupling reactions and collapsing model in the roasting process of recycling metals from LiCoO₂ batteries, J. Clean. Prod. 205 (2018) 923–929, <https://doi.org/10.1016/j.jclepro.2018.09.098>.

[36] M. Wang, Q. Tan, L. Liu, J. Li, A. Facile, Environmentally friendly, and low-temperature approach for decomposition of polyvinylidene fluoride from the cathode electrode of spent lithium-ion batteries, ACS Sustain. Chem. Eng. 7 (2019) 12799–12806, <https://doi.org/10.1021/acssuschemeng.9b01546>.

[37] L. Tian, X. Huang, X. Tang, Study on morphology behavior of PVDF-based electrolytes, J. Appl. Polym. Sci. 92 (2004) 3839–3842, <https://doi.org/10.1002/app.20402>.

[38] S. Windisch-Kern, A. Holzer, L. Wiszniewski, H. Raupenstrauch, Investigation of potential recovery rates of nickel, manganese, cobalt, and particularly lithium from NMC-Type cathode materials (Li_{Ni_xMn_yCo_zO₂) by Carbo-thermal reduction in an inductively heated carbon Bed Reactor, Metals 11 (2021) 1844, <https://doi.org/10.3390/met11111844>.}

[39] Y. Zheng, W. Song, W. Mo, L. Zhou, J.W. Liu, Lithium fluoride recovery from cathode material of spent lithium-ion battery, RSC Adv 8 (2018) 8990–8998, <https://doi.org/10.1039/C8RA00061A>.

[40] S. Kim, J.G. Alauzin, N. Louvain, N. Brun, L. Stievano, B. Boury, L. Monconduit, P. H. Mutin, Alginic acid aquagel as a template and carbon source in the synthesis of Li₄Ti₅O₁₂/C nanocomposites for application as anodes in Li-ion batteries, RSC Adv 8 (2018) 32558–32564, <https://doi.org/10.1039/C8RA05928D>.

[41] Md.S.A. Bhuyan, H. Shin, Fundamental investigation of direct cathode regeneration using chemically delithiated lithium cobalt oxides, J. Electrochem. Soc. 169 (2022) 110507, <https://doi.org/10.1149/1945-7111/ac9d68>.

[42] D. Mohanty, H. Gabrisch, Microstructural investigation of Li_{Ni_xMn_y3/Co_{1-x-y}O₂ (x ≤ 1) and its aged products via magnetic and diffraction study, J. Power Sources 220 (2012) 405–412, <https://doi.org/10.1016/j.jpowsour.2012.08.005>.}

[43] J. Landesfeind, A. Eldiven, H.A. Gasteiger, Influence of the binder on lithium ion battery electrode tortuosity and performance, J. Electrochem. Soc. 165 (2018) A1122–A1128, <https://doi.org/10.1149/2.0971805jes>.

[44] A. Mistry, S. Trask, A. Dunlop, G. Jeka, B. Polzin, P.P. Mukherjee, V. Srinivasan, Quantifying negative effects of carbon-binder networks from electrochemical performance of porous li-ion electrodes, J. Electrochem. Soc. 168 (2021) 070536, <https://doi.org/10.1149/1945-7111/ac1033>.

[45] M. Kroll, S.L. Karstens, M. Cronau, A. Höltzel, S. Schlabach, N. Nobel, C. Redenbach, B. Roling, U. Tallarek, Three-phase reconstruction reveals how the microscopic structure of the carbon-binder domain affects ion transport in lithium-ion batteries, Batter. Supercaps 4 (2021) 1363–1373, <https://doi.org/10.1002/batt.202100057>.

[46] J. Xiao, Q. Li, Y. Bi, M. Cai, B. Dunn, T. Glossmann, J. Liu, T. Osaka, R. Sugiura, B. Wu, J. Yang, J.G. Zhang, M.S. Whittingham, Understanding and applying coulombic efficiency in lithium metal batteries, Nat. Energy 5 (2020) 561–568, <https://doi.org/10.1038/s41560-020-0648-z>.

[47] R. Frech, Effect of propylene carbonate as a plasticizer in high molecular weight PEO-LiCF₃SO₃ electrolytes, Solid State Ion 85 (1996) 61–66, [https://doi.org/10.1016/0167-2738\(96\)00041-0](https://doi.org/10.1016/0167-2738(96)00041-0).

[48] S. Das, A. Ghosh, Ionic conductivity and dielectric permittivity of PEO-LiClO₄ solid polymer electrolyte plasticized with propylene carbonate, AIP Adv 5 (2015) 027125, <https://doi.org/10.1063/1.4913320>.

[49] H. Jia, H. Onishi, N. Von Aspern, U. Rodehorst, K. Rudolf, B. Billmann, R. Wagner, M. Winter, I. Cekic-Laskovic, A propylene carbonate based gel polymer electrolyte for extended cycle life and improved safety performance of lithium ion batteries, J. Power Sources 397 (2018) 343–351, <https://doi.org/10.1016/j.jpowsour.2018.07.039>.

[50] X. Huang, S. Zeng, J. Liu, T. He, L. Sun, D. Xu, X. Yu, Y. Luo, W. Zhou, J. Wu, High-performance electrospun poly(vinylidene fluoride)/Poly(propylene carbonate) gel polymer electrolyte for lithium-ion batteries, J. Phys. Chem. C 119 (2015) 27882–27891, <https://doi.org/10.1021/acs.jpcc.5b09130>.